AAC Journals.ASM.org

Biochemical Study of the Comparative Inhibition of Hepatitis C Virus RNA Polymerase by VX-222 and Filibuvir

Guanghui Yi,[a]* Jerome Deval,[b]* Baochang Fan,[a] Hui Cai,[a] Charlotte Soulard,[b] C. T. Ranjith-Kumar,[a] David B. Smith,[b] Lawrence Blatt,[b] Leonid Beigelman,[b] and C. Cheng Kao[a]

Department of Molecular and Cellular Biochemistry, Indiana University, Bloomington, Indiana, USA,[a] and Alios Biopharma, Inc., South San Francisco, California, USA[b]

Filibuvir and VX-222 are nonnucleoside inhibitors (NNIs) that bind to the thumb II allosteric pocket of the hepatitis C virus (HCV) RNA-dependent RNA polymerase. Both compounds have shown significant promise in clinical trials and, therefore, it is relevant to better understand their mechanisms of inhibition. In our study, filibuvir and VX-222 inhibited the 1b/Con1 HCV subgenomic replicon, with 50% effective concentrations (EC_{50}s) of 70 nM and 5 nM, respectively. Using several RNA templates in biochemical assays, we found that both compounds preferentially inhibited primer-dependent RNA synthesis but had either no or only modest effects on *de novo*-initiated RNA synthesis. Filibuvir and VX-222 bind to the HCV polymerase with dissociation constants of 29 and 17 nM, respectively. Three potential resistance mutations in the thumb II pocket were analyzed for effects on inhibition by the two compounds. The M423T substitution in the RNA polymerase was at least 100-fold more resistant to filibuvir in the subgenomic replicon and in the enzymatic assays. This resistance was the result of a 250-fold loss in the binding affinity (K_d) of the mutated enzyme to filibuvir. In contrast, the inhibitory activity of VX-222 was only modestly affected by the M423T substitution but more significantly affected by an I482L substitution.

Hepatitis C virus (HCV), the major causative agent of non-A, non-B viral hepatitis, has been estimated to infect over 170 million people worldwide (12, 24). Approximately 80% of the infected individuals will develop chronic infection, leading to liver cirrhosis and hepatocellular carcinoma (24). Two protease inhibitors have been recently approved by the FDA and can result in up to a 70% cure rate for genotype 1a- or 1b-infected patients when used in combination with pegylated alpha interferon and ribavirin (1, 17). However, resistance mutations to both ribavirin and the protease inhibitors have already been observed in patients, and there is a need to develop drugs to additional targets in HCV (3). The HCV-encoded NS5B, the RNA-dependent RNA polymerase (RdRp) (5), is a validated drug target, and intense efforts are focused on development of antiviral agents that inhibit its activities.

The HCV RdRp can catalyze RNA synthesis *in vitro* by either a *de novo*-initiated mechanism or by extension from a primed template (19, 40). These two modes of RNA synthesis have been used to classify the effects of HCV polymerase inhibitors (13). *De novo* initiation usually takes place by the base pairing of the initiating nucleoside triphosphate (NTP; usually a purine triphosphate) to the 3′-most nucleotide of the template RNA (usually a U or a C) (5, 19, 21, 30). This mode of synthesis ensures that no genetic information from the viral genome is lost (18). It is the rate-limiting step in RNA synthesis and requires a higher K_m of the initiating NTP (NTPi) than for the other nucleotides incorporated during elongation. Primer extension (PE) takes place when the 3′ region of the template RNA loops back on itself to form a hairpin structure or when a second RNA anneals to the first to provide an accessible 3′ terminus (5, 19). Functionally, PE mimics the elongative RNA synthesis by HCV without requiring the *de novo* initiation step (9). The two modes of RNA synthesis also require distinct conformations or oligomerization states of the polymerase (10).

Several nonnucleoside inhibitors (NNIs) of the HCV polymerase can prevent either *de novo*-initiated RNA synthesis, primer-extended RNA synthesis, or both. These NNIs bind to one of the four validated allosteric pockets in NS5B (3, 9, 31, 32). Two pockets are in the thumb domain and two in the palm domain. The palm I and palm II sites partially overlap and are close to the catalytic residues that bind the divalent metal ions. The NNI ANA-598 binds to the palm I pocket, and HCV-796 binding to the palm II pocket inhibits RNA synthesis (20, 22, 39). The thumb I domain binds benzimidazole and indole-based NNIs to inhibit RNA synthesis, while thiophene-2-carboxylates, dihydroxyprones, and phenylalanine derivatives bind to the thumb II pocket, a hydrophobic cleft in the thumb domain that is located about 30 Å from the catalytic site (Fig. 1B).

Although many small molecules have been reported to interact with the thumb II pocket, no specific analysis of the inhibition of *de novo* initiation has been reported (6, 7, 14, 16, 21, 23, 29, 38, 42). Filibuvir, also known as PF-00868554 (Fig. 1A), is a member of the dihydroxyprone class of compounds that was identified by a high-throughput screen and dihydroxyprone-based drug design efforts (26). Results from clinical phase 1b trial showed that filibuvir potently decreased viral RNA accumulation in a dose-dependent manner (http://clinicaltrials.gov/ct2/show/NCT00987337). Filibuvir has potent *in vitro* activity against genotype 1a and 1b replicons (2, 26, 37). The structure of filibuvir when cocrystallized with a 1b HCV polymerase revealed extensive contact between filibuvir and residues in the thumb II pocket, including hydrophobic interactions with residues L419, M423, Tyr477, and Trp528 (Fig. 1B) (26). Resistance to filibuvir is associated with substitu-

Received 1 August 2011 **Returned for modification** 29 September 2011
Accepted 23 November 2011
Published ahead of print 5 December 2011
Address correspondence to C. Cheng Kao, ckao@indiana.edu.
* G. Yi and J. Deval contributed equally to this work.
Copyright © 2012, American Society for Microbiology. All Rights Reserved.
doi:10.1128/AAC.05438-11

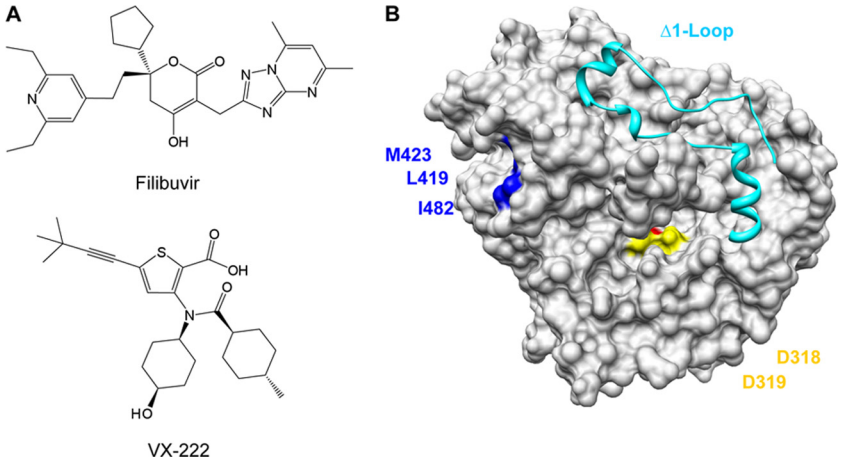

FIG 1 Structures of filibuvir and VX-222 (A) and the locations of three resistance mutations in the thumb II domain targeting the thumb allosteric binding site (B). The ribbon structure represents the Δ1 Loop, which covers the template channel of HCV RdRp.

tions in some of these residues in the thumb II pocket (41). VX-222 is a thiophene-2-carboxylic acid derivative that also targets the thumb II pocket of the HCV RNA polymerase (Fig. 1A). In phase 1b/2a trials, VX-222 decreased HCV levels by more than 3 logs when patients were treated with 250 to 750 mg twice daily or 1,500 mg once daily (4, 15, 36). HCV subgenomic replicons exposed to thiophene-2-carboxylic acid-based compounds yielded resistant replicon variants with mutations at residues L419, M423, and I482 in the thumb domain of the NS5B polymerase (25). No crystal structure of VX-222 bound to the HCV polymerase has, to our knowledge, been reported.

In this work, we show that both filibuvir and VX-222 preferentially inhibit elongative RNA synthesis rather than *de novo*-initiated RNA synthesis. Furthermore, the resistance mutations in residues L419, M423, and I482 had different effects on the level of inhibition of RNA synthesis by the polymerase in the presence of filibuvir or VX-222. Our results support the idea that filibuvir and VX-222 occupy partially overlapping but not identical binding sites.

MATERIALS AND METHODS

Compounds. Filibuvir and ANA-598 were obtained from Acme Bioscience, Inc. (Palo Alto, CA), and VX-222 was obtained from Sellect Chem (Houston, TX). The compounds were dissolved in 100% dimethyl sulfoxide (DMSO) at a final concentration of 10 mM and stored at −80°C until use.

HCV replicons. Mutant HCV replicons were made by site-directed mutagenesis using the genotype 1b/Con1 wild-type replicon pFKI389/NS3-3′/WT as template (28). All mutations were confirmed by sequencing of both DNA strands. To generate transcripts for replicons, plasmids containing the replicons were linearized with ScaI, purified by using a Qiagen column, and then employed for *in vitro* transcription with the AmpliScribe T7-Flash transcription kit (Epicentre Technologies).

Huh7.5 cell lines were made to stably express WT and mutant HCV replicons. The cells were maintained in Dulbecco's modified Eagle medium supplemented with 10% fetal bovine serum, 100 U of penicillin-streptomycin/ml, and 0.1 mM nonessential amino acids. Trypsinized Huh7.5 cells were washed twice with ice-cold Cytomix (120 mM KCl, 0.15 mM $CaCl_2$, 10 mM K_2HPO_4/KH_2PO_4, 25 mM HEPES, 2 mM EGTA, 5 mM $MgCl_2$; pH 7.6) and suspended at 1×10^7 cells/ml in ice-cold Cytomix. A 200-μl volume of the cell suspension, 5 μg HCV replicon RNA, and 5 μg carrier RNA (total RNA extracted from naïve Huh7.5 cells) was transferred to an electroporation cuvette with a 2-mm gap and pulsed at 270 V, 960 μF to introduce the RNAs (Bio-Rad Gene Pulser). The cells were allowed to recover at room temperature for 10 min before dilution in complete medium. Twenty-four hours after electroporation, G418 (Invitrogen) was added to the medium, and the cells were maintained in the selective medium (replaced every 3 days) until the isolation of replicon-harboring colonies approximately 3 weeks after transfection. The expression of HCV NS5A protein in these cells was confirmed by an immunofluorescence assay with antibody from Santa Cruz Biotechnology.

EC_{50} determinations with HCV replicon-expressing cells. Huh7.5 cells harboring replicons were trypsinized and plated into 48-well plates at 40,000 cells/well. The next day the medium was changed and inhibitors were added to the cells at seven different concentrations, each pair of which differed by 3- or 10-fold dilutions in 200 μl complete medium with triplicates. After 48 h, total RNA was extracted from replicon cells using the TRIzol reagent (Invitrogen), and viral RNAs were quantified by real-time reverse transcription-PCR (RT-PCR). First-strand cDNA synthesis used 1 μg of total RNA along with Moloney murine leukemia virus (NEB) and 4 μM randomized 9-nucleotide (nt) primer mix. RT-PCR used the Bio-Rad IQ SYBR green kit (Bio-Rad), and primers were HCV 5′-UTRsense (5′-AGC CAT GGC GTT AGT ATG AGT GTC-3′) and 5′-UTRanti (5′-ACA AGG CCT TTC GCG ACC CAA C-3′). Glyceraldehyde-3-phosphate dehydrogenase (GAPDH) was detected using the sense and antisense oligonucleotides 5′-GAG TCA ACG GAT TTG GTC GT-3′ and 5′-TGG GAT TTC CAT TGA TGA CA-3′, respectively. All reaction mixtures were heated to 95°C for 10 min, followed by 40 cycles of PCR of 15 s at 95°C, 20 s at 55°C, and 30 s at 72°C. The fold change and percent change of each group were compared to values for controls as previously described (27). The effective drug concentrations that reduced HCV RNA replicon levels by 50% (EC_{50}s) were calculated with GraphPad Prism software by nonlinear regression analysis with log curve fitting.

Expression and purification of recombinant HCV polymerases. The HCV NS5B protein lacking the C-terminal 21 amino acids, named 1bΔ21, was cloned in pET-21b as described previously (11). The construct contains a C-terminal six-histidine tag to facilitate protein purification. L419M, M423T, and I482L resistance mutants were made by site-directed mutagenesis from the WT 1bΔ21 expression plasmid. Recombinant 1bΔ21 and the mutant proteins derived from 1bΔ21 were expressed and purified from *Escherichia coli* extract by using Talon metal affinity resin (Clontech) followed by a Mono S column (Pharmacia) as described by Chinnaswamy et al. (10). Protein concentrations were quantified by use of a nanodrop spectrophotometer followed by checks for purity and protein concentration using SDS-PAGE and a titration series with bovine serum albumin.

Gel-based RdRp assay with small RNA templates. RdRp assays were carried out in 20-μl reaction mixtures containing 20 mM sodium glutamate (pH 8.2), 12.5 mM dithiothreitol, 4 mM $MgCl_2$, 1 mM $MnCl_2$, 0.5% Triton X-100, 0.2 mM GTP, 0.1 mM ATP and UTP, 3.3 nM [α-^{32}P]CTP (MP Biomedicals), 40 nM recombinant RNA polymerases, 100 nM PE46, 50 nM LE19p. The reaction mixture was incubated at 30°C for 1 h, and the reaction was stopped by phenol-chloroform extraction, followed by ethanol precipitation of the RNA in the presence of 5 μg glycogen and 0.3 M NaO-acetate (pH 5.2). RNA products were separated by 7.5 M urea–20% polyacrylamide gels. The signal was detected by a PhosphorImager and quantified with the ImageQuant software. The 50% inhibitory concentration (IC_{50}) was calculated with GraphPad Prism software by nonlinear regression analysis with log curve fitting.

Filter plate RdRp assay with long RNA templates. The enzymatic reaction was performed in a 50-μl volume in 96-well plates (21). Each well contained 50 nM 1bΔ21, 0.5 μCi [^{3}H]UTP, and either 50 nM cIRES single-stranded RNA or 5 μM poly(A)-oligo$(dT)_{18}$ that served as templates for RNA synthesis. The reaction used MADV 96-well filter plates (Millipore) and were incubated for 2 h at 30°C. Each reaction was stopped by adding trichloroacetic acid to 10% (vol/vol), followed by incubation at 4°C for 40 min and filtration. Radiolabel was quantified in vials containing 40 μl of Microscint-20 in a Topcount microplate reader (Perkin-Elmer). The IC_{50} (50% reduction in radioactivity relative to untreated control) was determined using a nonlinear fit (GraphPad Prism).

DSF. Differential scanning fluorimetry (DSF) was performed in a Stratagene MX3005P real-time PCR machine. Each sample was prepared in a total volume of 25 μl that contained a 5× final concentration of SYPRO orange (Molecular Probes) in buffer T (100 mM Tris [pH 7.0], 160 mM NaCl, and 5 mM $MgCl_2$) and a molar excess of polymerase inhibitors relative to polymerase. All the samples were heated at a rate of 0.5°C/min, from 25 to 75°C, and the fluorescence intensity data were analyzed by GraphPad Prism.

Surface plasmon resonance. All analyte binding experiments were performed with a Biacore T100 instrument using preconditioned CM5 sensor chips activated with *N*-hydroxysuccinimide ester and 1-ethyl-3(3-diaminopropyl) carbodiimide hydrochloride. The 1bΔ21 NS5B protein and variants were immobilized after a 5-min injection to a nominal density of about 9,000 response units. The surface was then deactivated by injection of ethanolamine for 7 min. Compounds were injected in a buffer containing 25 mM HEPES (pH 7.4), 10 mM $MgCl_2$, 150 mM NaCl, 0.01% Tween 20, 0.05% β-mercaptoethanol, and 5% DMSO. All compounds displayed saturable 1:1 binding behavior. For competition binding, the experimental design consisted of injecting a saturating concentration of the first analyte (160 nM filibuvir) followed by immediate injection of an equimolar ratio of the analyte mixture (160 nM filibuvir plus 160 nM VX-222 or ANA-598).

RESULTS AND DISCUSSION

Characterization of replicon resistance mutants targeting the thumb II domain. Filibuvir and VX-222 are promising inhibitors of the HCV RNA polymerase. Therefore, the goal of this study was to better understand their mechanisms of action. We first sought to confirm the effects of the inhibitors in Huh7.5 cells that expressed the WT replicon or replicons with potential resistance mutations. Three 1b Con1-derived replicons with mutations in the thumb II pocket, M423T, I482L, and L419M, were selected for further characterization, since they were previously reported to confer resistance to thiophene-2-carboxylates and were also observed in the presence of filibuvir, VX-222, or both compounds (25, 37). In the absence of these compounds, the mutant replicons grew similarly to the WT (Fig. 2A) DNA sequencing demonstrated that the engineered mutations were retained for at least seven passages (data not shown).

To determine the EC_{50}s of filibuvir and VX-222, cell lines harboring the HCV replicon were treated with increasing concentrations of the inhibitors followed by quantification of the viral RNA 48 h later using real-time RT-PCR (Fig. 2A). In the presence of filibuvir, the WT 1b replicon was inhibited in a dose-dependent manner, with an EC_{50} of ~70 nM (Fig. 2B and C), in good agreement with the reported EC_{50} of 41 nM (26). VX-222 had an EC_{50} of ~5 nM, also in good agreement with the reported EC_{50} of 12 nM (15). A control for specificity in this experiment, ANA-598, which targets the palm I pocket, had an EC_{50} of 1.2 nM. The effects of the three inhibitors were also examined in a luciferase-expressing HCV replicon, and the EC_{50} results detected by luciferase levels were highly consistent with those from real-time RT-PCR (data not shown).

Mutant replicons (L419M, M424T, and I482L) were individually tested with filibuvir, VX-222, and ANA-598. ANA-598 had comparable EC_{50}s against the WT and the three mutant replicons, as was expected (Fig. 2B and C). For filibuvir, mutant M423T had an EC_{50} higher than 10 μM, a 142-fold increase above that of the WT replicon. The I482L replicon was only moderately resistant to filibuvir, with a 5-fold increase in the EC_{50} (Fig. 2C). Filibuvir had an EC_{50} of 225 nM against the L419M mutant, which was only 3-fold higher than against the WT. These results confirm previous observations that M423T is the predominant resistance mutation for filibuvir in cell culture and in clinically treated patients (37, 41).

The three resistance mutations all had some effects on resistance to VX-222. The I482L replicon had the most dramatic effect on inhibition by VX-222, increasing the EC_{50} approximately 100-fold above that for the WT. The M423T and L419M replicons had more modest 15- and 9-fold higher EC_{50}s compared to the WT (Fig. 2C). The three residues in the thumb II pocket contribute differently to the resistance of VX-222 and filibuvir.

Inhibition of RNA synthesis in biochemical assays with filibuvir and VX-222. The HCV RNA polymerase can direct RNA synthesis *in vitro* by either a *de novo*-initiated mechanism or by extension from a primed template (34). Whether filibuvir and VX-222 differentially affect these two modes of RNA synthesis *in vitro* was examined with a gel-based RdRp assay. The LE19P RNA template, which was able to direct *de novo* initiation has a modified 3′ terminus to block primer extension, resulted in a 19-nt RNA product (10) (Fig. 3A). PE46 is designed to form a partial RNA hairpin, where the 3′-terminal residue is base paired. The RNA extended from PE46 is 46 nt in length. ANA-598 inhibited both *de novo* RNA synthesis and primer extension in a concentration-dependent manner, with IC_{50}s between 4 and 5 nM (Fig. 3B and Table 1).

Filibuvir had no obvious effect on *de novo*-initiated RNA synthesis but decreased primer extension from PE46, with an IC_{50} of 73 nM (Fig. 3B and Table 1). VX-222 reduced *de novo* initiation slightly but also showed strong inhibition of primer extension. The IC_{50} for filibuvir inhibition of *de novo*-initiated RNA synthesis was ~5 μM (Fig. 3B and Table 1). HCV-796 affected both *de novo* initiation and primer extension equally, while ANA-598 preferentially inhibited *de novo*-initiated RNA synthesis and also inhibited primer extension (Fig. 3B). The IC_{50} of VX-222 for primer-extended RNA synthesis was 31 nM. The preferential inhibition of elongative RNA synthesis by filibuvir and VX-222 suggests a different mode of inhibition than with HCV-796 and ANA-598.

To confirm these results, we use a partially duplexed

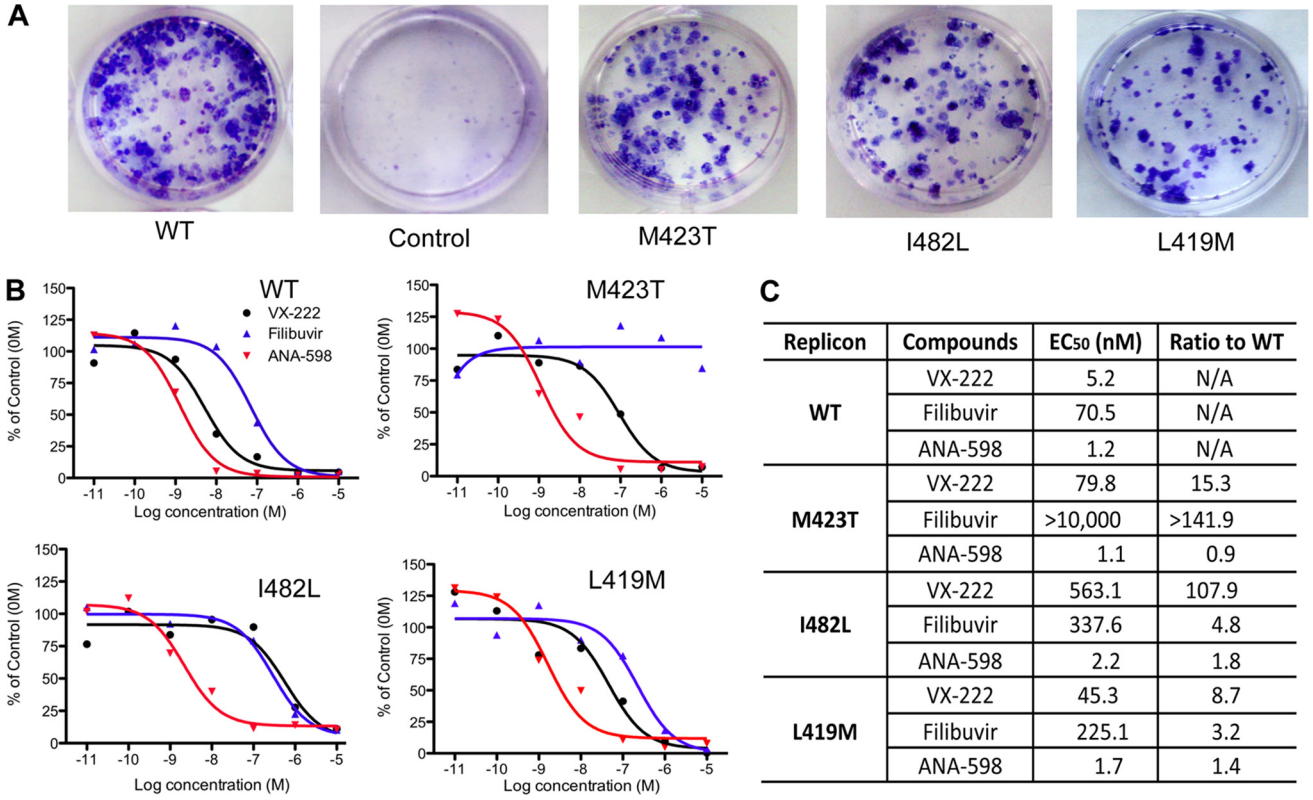

C

Replicon	Compounds	EC_{50} (nM)	Ratio to WT
WT	VX-222	5.2	N/A
	Filibuvir	70.5	N/A
	ANA-598	1.2	N/A
M423T	VX-222	79.8	15.3
	Filibuvir	>10,000	>141.9
	ANA-598	1.1	0.9
I482L	VX-222	563.1	107.9
	Filibuvir	337.6	4.8
	ANA-598	2.2	1.8
L419M	VX-222	45.3	8.7
	Filibuvir	225.1	3.2
	ANA-598	1.7	1.4

FIG 2 Effects of filibuvir, VX-222, and ANA-598 on the EC_{50}s of HCV replicons. (A) Foci formation by the WT 1b/Con1 and mutant replicons. The cells were stained with crystal violet, and comparable dilutions of transfected Huh7.5 cells are shown. (B) Sample data observed for the EC_{50} of WT and three mutant replicons in the presence of NNIs. Seven-log dilutions (from 0.01 nM to 10 μM) were tested, each in triplicate. The HCV RNA was quantified by real-time PCR as described in Materials and Methods. (C) Summary of the EC_{50}s and fold changes in the EC_{50}s of the three mutants relative to the WT.

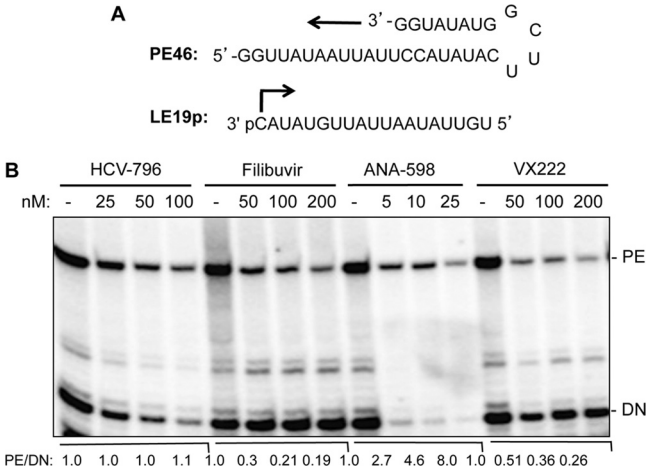

FIG 3 Effects of nonnucleoside analog inhibitors on RNA synthesis by the recombinant HCV RdRp. (A) Sequence of RNA templates used in the gel-based RNA synthesis assay. PE46 was designed to form a partially duplexed RNA that can be extended from its 3′ terminus to form a 46-nt RNA product. LE19P, a 19-nt RNA that contains a 3′-terminal puromycin, can direct *de novo*-initiated RNA synthesis from the 3′-terminal cytidylate and results in a 19-nt product. (B) *In vitro* RdRp assay with increased concentrations of filibuvir, ANA-598, and VX-222. The RNA product was separated on a 20% polyacrylamide–7.5 M urea gel, and the radioactive signal was detected and quantified using a PhosphorImager. The *de novo*-initiated product (DN) is identified to the right of the gel image. The primer-extended product (PE) is also identified. For each of the four treatments, the ratios of the PE to the *de novo*-initiated products were calculated relative to the samples that were mock treated with the carrier to the compounds.

oligo$(dT)_{18}$ primer annealed to heterogeneous poly(A) template molecules to monitor primer extension. The IC_{50} in this reaction was 50 nM for filibuvir and 11 nM for VX-222 (Table 1), values that are similar to those obtained with the PE46 template. To examine *de novo* initiation activity, we used a transcript containing the 3′ portion of the minus-strand HCV, named cIRES, that is capable of *de novo*-initiated RNA synthesis as well as some primer extension (35). For filibuvir, no obvious inhibitory effect was observed at a 10 μM final concentration, while for VX-222 the IC_{50} was about 150 nM, ~10-fold higher than the value for poly(A)-oligo$(dT)_{18}$ (Table 1). Preincubation of either filibuvir or VX-222 with the enzyme for 15 min before the addition of the NTPs and poly(A)-oligo$(dT)_{18}$ did not alter the inhibition of RNA synthesis significantly (data not shown). The results with the poly(A)-oligo$(dT)_{18}$ and cIRES templates are consistent with primer elongative RNA synthesis being inhibited by filibuvir and VX-222. In contrast, ANA-598 retained its potency under all of the tested conditions.

Mutations in the thumb II pocket affected inhibition by filibuvir and VX-222. To determine whether mutations in NS5B are sufficient to confer resistance to filibuvir and VX-222, we expressed and purified recombinant 1bΔ21 polymerases with the L419M, I482L, and M423T substitutions. All three mutant polymerases were active for RNA synthesis by both *de novo* initiation and primer extension (Fig. 4A). In the DSF assay (33), the denaturation profiles of the three mutants were indistinguishable from that of 1bΔ21, even when protein concentration varied over a

TABLE 1 IC_{50}s of filibuvir, VX-222, and ANA-598 for RNA synthesis by 1bΔ21 from five different templates

Template	Mean IC_{50} in μM (*n*)[a]			
	Filibuvir	VX-222	ANA-598	HCV-796
Poly(rA)-oligo$(dT)_{18}$	0.05 ± 0.027 (6)	0.011 ± 0.005 (4)	0.005 ± 0.004 (4)	
Poly(I/C)	0.4 (2)	0.016 (1)	0.003 (1)	
cIRES	>10 (2)	0.15 (2)	0.006 (2)	
PE46	0.073 ± 0.051 (4)	0.031 ± 0.011 (4)	0.005 (2)	0.013 (1)
LE19P	>50 (4)	>5 (4)	0.004 (2)	0.010 (1)

[a] For some templates, the standard error of the mean is also provided. *n* is the number of data sets.

10-fold range in the assay (Fig. 4B). In addition, all three mutant proteins were inhibited by ANA-598, with IC_{50}s similar to that of 1bΔ21 (Fig. 4C). These results suggest that the mutations did not grossly change the conformation or the oligomerization states of the mutant enzymes relative to 1bΔ21, and such information should allow us to interpret and compare results of the effects of the inhibitors.

The IC_{50} for the M423T mutant with filibuvir using the poly(A)-oligo$(dT)_{18}$ template was 600-fold higher than that of 1bΔ21 (Fig. 4C). Mutant proteins L419M and I482L increased the IC_{50} by only up to 6-fold. Identical trends were observed in reactions performed with the template PE46. These results confirmed the observation that M423 in the 1b HCV polymerase is critical for inhibition by filibuvir. The mutation-induced phenotype against VX-222 was different. All three of the substitutions increased the IC_{50} from 5- to 29-fold with poly(rA)-oligo$(dT)_{18}$ and between 3- and 10-fold with PE46.

Filibuvir and VX-222 binding to the HCV polymerase. The results from the *in vitro* RNA synthesis assays suggested that binding of VX-222 or filibuvir to the polymerase should be affected by the resistance mutations. DSF (33), which can demonstrate protein binding to ligands, was used in our initial analysis. Filibuvir present at a range from a molar ratio of 1- to 10-fold excess of the polymerase monomer caused an increase in the apparent melting point [$T_{m(app)}$] of 1bΔ21, demonstrating that the compound binds to the polymerase (Fig. 5A and data not shown). With a 1.2-to-1 ratio of filibuvir to 1bΔ21, the $T_{m(app)}$ change was 2.5°C.

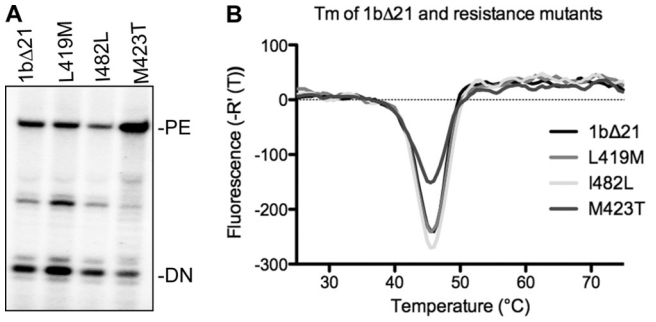

C

Template:	poly(rA)/dT18			PE46	
	ANA-598	Filibuvir	VX-222	Filibuvir	VX-222
L419M	1	6	29	2.4	2.8
I482L	2	5	14	2.4	10
M423T	0.5	600	4.5	>100	6.3

FIG 4 Examination of RNA synthesis by mutant HCV RdRps. (A) Products made by the WT and mutant polymerases, with LE19 and PE46 as the templates. (B) Results from DSF spectroscopy of 1bΔ21 and the three mutant polymerases. Between 2.5 and 5 μg of the four proteins was used in the assay, and the temperature observed for the greatest change in fluorescence [$T_{m(app)}$] is shown. (C) RNA synthesis by the mutant polymerase in the presence of ANA-598, filibuvir, or VX-222. Two primer extension templates were used, and the resulting IC_{50}s were compared to those from 1bΔ21 (reported as the fold change). The IC_{50}s for 1bΔ21 with ANA-598, filibuvir, and VX-222 were 5 nM, 50 nM, and 11 nM with the duplex of poly(rA)-oligo$(dT)_{18}$. The IC_{50}s of filibuvir and VX-222 with 1bΔ21 were 73 nM and 31 nM with PE46, as documented in Table 1.

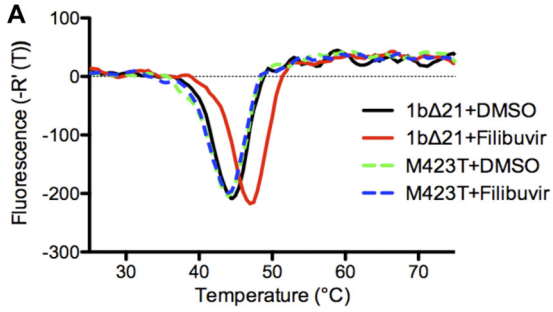

C

	1bΔ21	M423T	I482L	L419M
DMSO:	44.5	44.3	44.25	44.75
Filibuvir:	47.0	44.5	46.7	46.1
ΔTm_{app}:	2.5	0.2	2.45	1.35
VX-222:	48.0	47.0	47.0	47.0
ΔTm_{app}:	3.5	2.7	2.75	2.25

FIG 5 Examination of filibuvir or VX-222 binding based on DSF spectroscopy. (A) Derivatives of the thermal denaturation profiles of 1bΔ21 and M423T in the presence of filibuvir. The molar ratio of filibuvir to the proteins is 1.2. DMSO was used as a vehicle control and was present in the reaction mixture at a final concentration of 4%. Each curve was derived from the mean value of three independent samples. The samples within a set had $T_{m(app)}$s that varied less than 0.2°C. (B) Derivatives of the thermal denaturation profiles of 1bΔ21 and I482L in the presence of VX-222. (C) Summary of the effects of filibuvir and VX-222 on the $T_{m(app)}$ of the 1bΔ21 and the three mutant proteins with substitutions in the thumb II pocket.

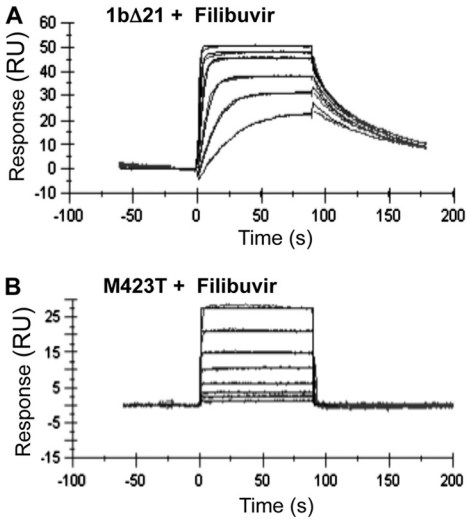

C

	1bΔ21		M423T		I482L	L419M
	VX-222	Filibuvir	VX-222	Filibuvir	Filibuvir	Filibuvir
K_d (nM):	17	29	17	7300	133	46
K_{on} ($M^{-1}S^{-1}$):	6.3e5	1.1e6	2.3e6	1.5e4	N.D.	2.3e6
K_{off} (S-1):	0.011	0.033	0.040	0.11	N.D.	0.12

FIG 6 Binding affinities and kinetics for filibuvir and VX-222 by SPR. The 1bΔ21 protein (WT or mutant) was immobilized on the surface of the biosensor CM5 chip (Biacore) by amine coupling. (A) Sensorgram of filibuvir binding to immobilized 1bΔ21. A representative sensorgram is shown for six analyte concentrations (0.8, 0.4, 0.2, 0.1, 0.05, and 0.025 μM) injected for 90 s each. (B) The same experiment as shown in panel A, but with the M423T mutant and concentrations of filibuvir of 30, 15, 7.5, 3.8, 1.9, 0.94, 0.47, and 0.23 μM. (C) A summary of the binding affinity (K_d) on and off rates for VX-222 and filibuvir for 1bΔ21 and the three resistance mutations. The results were derived from kinetic fit, using a 1:1 binding model (Biacore T100 Evaluation software; GE Healthcare).

Filibuvir at even up to a 10 molar ratio to the M423T polymerase did not exhibit this change (Fig. 5A and data not shown). L419M had a 1.4°C change in the $T_{m(app)}$ in the presence of filibuvir, while no obvious difference was observed with the I482L mutant protein (Fig. 5C). With VX-222, 1bΔ21 had a higher $T_{m(app)}$ by 3.5°C (Fig. 5B). Consistent with all three mutant polymerases being moderately affected for RNA synthesis, all three had decreased changes in their $T_{m(app)}$ (from 2.3 to 2.8°C) in the presence of VX-222 (Fig. 5C). These results suggest that all three residues contribute to VX-222 binding.

Surface plasmon resonance (SPR) was used to determine the binding affinity of filibuvir and VX-222 to the 1bΔ21 polymerase. The protein was immobilized on the surface of the biosensor chip through covalent amine coupling, and increasing concentrations of compounds were injected for 90 s each. Analysis of SPR sensorgrams showed that all compounds displayed saturable 1:1 binding behavior. Filibuvir bound to the 1bΔ21 with a K_d of 29 nM, a rapid "on" rate (6.3×10^5 M^{-1} s^{-1}) and a relatively slow "off" rate (0.011 s^{-1}) (Fig. 6A and C). VX-222 had a K_d of 17 nM, with on and off rate kinetics comparable to those of filibuvir. The M423T mutation marginally affected the binding affinity to VX-222. However, it resulted in a 250-fold increase in the K_d for filibuvir (Fig. 6B and C). The decreased binding affinity was due to a combined alteration of the on and off rate kinetics. Mutants I482L and L419M also exhibited modest defects in binding filibuvir, with K_ds of 133 nM and 46 nM, 4.6- and 1.6-fold above that of 1bΔ21. By using a tryptophan fluorescence-quenching method, we were able to confirm these changes in binding affinity for filibuvir with the three mutant proteins (data not shown). Overall, these results provide supporting evidence that the M423T mutation is a major contributor to the loss of binding affinity toward filibuvir, while I482L and L419M have more limited effects.

Finally, we conducted a series of SPR experiments to investigate the competitive nature of binding between filibuvir and VX-222. When we injected VX-222 onto NS5B protein already saturated with filibuvir, we observed no increase in the response, indicating no binding of VX-222 (Fig. 7A). In comparison, an

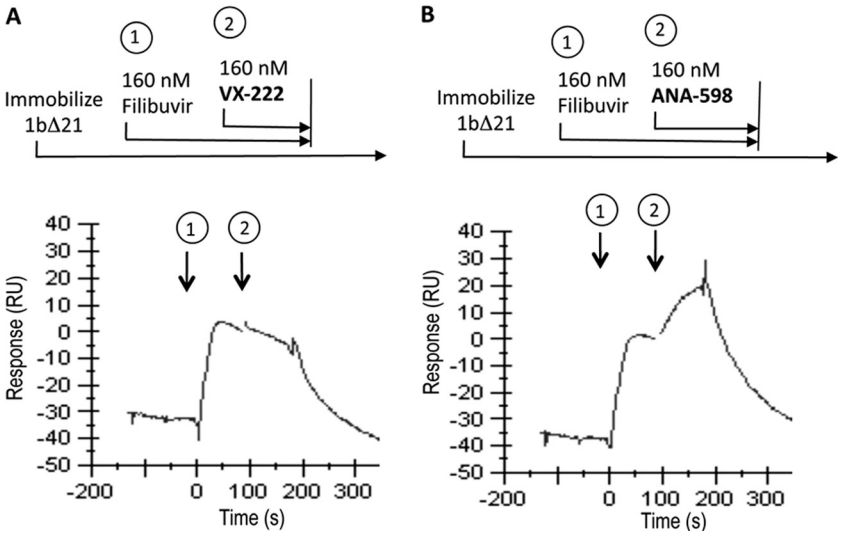

FIG 7 Competition binding experiments. The NS5B protein was immobilized to the surface of the SPR chip as previously described. Analytes were tested in dual injection mode, and the *y* axis was normalized at the beginning of the second injection. (A) First injection (1) for 90 s with 160 nM filibuvir, followed by a second 90-s injection (2) containing 160 nM filibruvir plus 160 nM VX-222. (B) Response after injection (1) for 90 s with 160 nM filibruvir, followed by a second 90-s injection (2) containing 160 nM filibruvir plus 160 nM ANA-598.

injection of ANA-598 resulted in an increase in binding signal even in the presence of saturating filibuvir (Fig. 7B). Based on this experiment and on the resistance profile, we conclude that filibuvir and VX-222 occupy at least a partially overlapping binding site.

Conclusions. We characterized the interaction of filibuvir and VX-222 with the thumb II pocket of the HCV polymerase and determined their effects on 1b/Con1 replicons as well as the polymerase activity. Both filibuvir and VX-222 have binding affinities (K_ds) for the HCV polymerase in the nanomolar range, with rapid on rates and relatively slow off rates. In the crystal structure of the filibuvir-polymerase complex (26, 37), L419 and I482 interact with the pyridine group, while M423 interacts with the cyclopentyl portion of the lactone. Our results show that the latter interaction is more important for stable binding by filibuvir. For VX-222, the crystal structure of the complex is not known, but all three residues we examined contributed to interaction with VX-222. We note that L412, M423, and I482 all help to form a hydrophobic surface within the thumb II domain, and it is likely that they interact hydrophobically with VX-222, likely with the 4-methycyclohexanoyl group.

Studies with inhibitors have demonstrated that the thumb subdomain has an important role in regulating the mode of RNA synthesis. Benzimidazole-based compounds that bind to the thumb I pocket likely affect the interaction between the Δ1 loop and the thumb subdomain to prevent *de novo*-initiated RNA synthesis (8, 11, 38). Chinnaswamy et al. (11) previously showed that a substitution in the thumb I subdomain can affect the interaction between subunits of the polymerase that are needed for *de novo*-initiated RNA synthesis. The results here with filibuvir and VX-222 and those of Le Pogam et al. (25) with thiophene-based compounds consistently reveal an inhibitory effect on the ability of the HCV polymerase to extend from a primed template. It is quite likely that the thumb region of the polymerase is involved in conformational changes and/or oligomerization states of the HCV polymerase that could regulate the activities of the polymerase, as proposed by Wang et al. (42). Furthermore, VX-222 and filibuvir likely interfere with the required conformational changes required for elongative RNA synthesis. DSF results did show a significant change in polymerase stability indicative of a conformational change (Fig. 4), but additional structural and functional analyses are needed to define the polymerase conformation(s) that could facilitate *de novo*-initiated or elongative RNA synthesis.

ACKNOWLEDGMENTS

We thank members of the Kao lab and Alios Biopharma for helpful discussions during this work.

C.C.K. acknowledges funding from NIAID grants RAI075015A and 1RO1AI073335.

REFERENCES

1. **Bacon BR, et al.** 2011. Boceprevir for previously treated chronic HCV genotype 1 infection. N. Engl. J. Med. **364**:1207–1217.
2. **Beaulieu PL.** 2010. Filibuvir, a non-nucleoside NS5B polymerase inhibitor for the potential oral treatment of chronic HCV infection. IDrugs **13**:938–948.
3. **Beaulieu PL.** 2009. Recent advances in the development of NS5B polymerase inhibitors for the treatment of hepatitis C virus infection. Expert Opin. Ther. Pat. **19**:145–164.
4. **Bedard J, et al.** 2009. Identification and characterization of VCH-222, a novel potent and selective non-nucleoside HCV polymerase inhibitor. Summ. 44th Annu. Meet. Eur. Assoc. Study Liver. EASL, Geneva, Switzerland. http://www.natap.org/2009/EASL/EASL_70.htm.
5. **Behrens SE, Tomei L, De Francesco R.** 1996. Identification and properties of the RNA-dependent RNA polymerase of hepatitis C virus. EMBO J. **15**:12–22.
6. **Biswal BK, et al.** 2005. Crystal structures of the RNA-dependent RNA polymerase genotype 2a of hepatitis C virus reveal two conformations and suggest mechanisms of inhibition by non-nucleoside inhibitors. J. Biol. Chem. **280**:18202–18210.
7. **Biswal BK, et al.** 2006. Non-nucleoside inhibitors binding to hepatitis C virus NS5B polymerase reveal a novel mechanism of inhibition. J. Mol. Biol. **361**:33–45.
8. **Bressanelli S, Tomei L, Rey FA, De Francesco R.** 2002. Structural analysis of the hepatitis C virus RNA polymerase in complex with ribonucleotides. J. Virol. **76**:3482–3492.
9. **Chinnaswamy S, Cai H, Kao C.** 2010. An update on small molecule inhibitors of the HCV NS5B polymerase: effects on RNA synthesis in vitro and in cultured cells. Virus Adapt. Treat. **2**:73–89.
10. **Chinnaswamy S, Murali A, Li P, Fujisaki K, Kao CC.** 2010. Regulation of de novo-initiated RNA synthesis in hepatitis C virus RNA-dependent RNA polymerase by intermolecular interactions. J. Virol. **84**:5923–5935.
11. **Chinnaswamy S, et al.** 2008. A locking mechanism regulates RNA synthesis and host protein interaction by the hepatitis C virus polymerase. J. Biol. Chem. **283**:20535–20546.
12. **Choo QL, et al.** 1989. Isolation of a cDNA clone derived from a blood-borne non-A, non-B viral hepatitis genome. Science **244**:359–362.
13. **De Francesco R, Migliaccio G.** 2005. Challenges and successes in developing new therapies for hepatitis C. Nature **436**:953–960.
14. **Di Marco S, et al.** 2005. Interdomain communication in hepatitis C virus polymerase abolished by small molecule inhibitors bound to a novel allosteric site. J. Biol. Chem. **280**:29765–29770.
15. **Highleyman L.** 2010. HCV polymerase inhibitor VX-222 demonstrates good safety and antiviral activity in treatment-naïve type 1 hepatitis C patients. Summ. 45th Annu. Meet. Eur. Assoc. Study Liver. EASL, Geneva, Switzerland. http://www.hivandhepatitis.com/2010_conference/easl/docs/0420_2010_c.html.
16. **Howe AY, et al.** 2006. Molecular mechanism of a thumb domain hepatitis C virus nonnucleoside RNA-dependent RNA polymerase inhibitor. Antimicrob. Agents Chemother. **50**:4103–4113.
17. **Jacobson IM, et al.** 2011. Telaprevir for previously untreated chronic hepatitis C virus infection. N. Engl. J. Med. **364**:2405–2416.
18. **Kao CC, Del Vecchio AM, Zhong W.** 1999. De novo initiation of RNA synthesis by a recombinant Flaviviridae RNA-dependent RNA polymerase. Virology **253**:1–7.
19. **Kao CC, et al.** 2000. Template requirements for RNA synthesis by a recombinant hepatitis C virus RNA-dependent RNA polymerase. J. Virol. **74**:11121–11128.
20. **Kirkovsky L, et al.** 2007. Preclinical characterization of a novel, potent, and pharmacokinetically appealing non-nucleoside inhibitor of HCV NS5B polymerase. 58th Annu. Meet. Am. Assoc. Study Liver Dis.
21. **Klumpp K, et al.** 2006. The novel nucleoside analog R1479 (4′-azidocytidine) is a potent inhibitor of NS5B-dependent RNA synthesis and hepatitis C virus replication in cell culture. J. Biol. Chem. **281**:3793–3799.
22. **Kneteman NM, et al.** 2009. HCV796: A selective nonstructural protein 5B polymerase inhibitor with potent anti-hepatitis C virus activity in vitro, in mice with chimeric human livers, and in humans infected with hepatitis C virus. Hepatology **49**:745–752.
23. **Kukolj G, et al.** 2005. Binding site characterization and resistance to a class of non-nucleoside inhibitors of the hepatitis C virus NS5B polymerase. J. Biol. Chem. **280**:39260–39267.
24. **Lauer GM, Walker BD.** 2001. Hepatitis C virus infection. N. Engl. J. Med. **345**:41–52.
25. **Le Pogam S, et al.** 2006. Selection and characterization of replicon variants dually resistant to thumb- and palm-binding nonnucleoside polymerase inhibitors of the hepatitis C virus. J. Virol. **80**:6146–6154.
26. **Li H, et al.** 2009. Discovery of (R)-6-cyclopentyl-6-(2-(2,6-diethylpyridin-4-yl)ethyl)-3-((5,7-dimethyl-[1,2,4]triazolo[1,5-a]pyrimidin-2-yl)methyl)-4-hydroxy-5,6-dihydropyran-2-on e (PF-00868554) as a potent and orally available hepatitis C virus polymerase inhibitor. J. Med. Chem. **52**:1255–1258.
27. **Livak KJ, Schmittgen TD.** 2001. Analysis of relative gene expression data using real-time quantitative PCR and the $2(-\Delta\Delta C_T)$ method. Methods **25**:402–408.

28. **Lohmann V, et al.** 1999. Replication of subgenomic hepatitis C virus RNAs in a hepatoma cell line. Science **285**:110–113.
29. **Love RA, et al.** 2003. Crystallographic identification of a noncompetitive inhibitor binding site on the hepatitis C virus NS5B RNA polymerase enzyme. J. Virol. **77**:7575–7581.
30. **Luo G, et al.** 2000. De novo initiation of RNA synthesis by the RNA-dependent RNA polymerase (NS5B) of hepatitis C virus. J. Virol. **74**: 851–863.
31. **Ma H, et al.** 2005. Inhibition of native hepatitis C virus replicase by nucleotide and non-nucleoside inhibitors. Virology **332**:8–15.
32. **McKercher G, et al.** 2004. Specific inhibitors of HCV polymerase identified using an NS5B with lower affinity for template/primer substrate. Nucleic Acids Res. **32**:422–431.
33. **Niesen FH, Berglund H, Vedadi M.** 2007. The use of differential scanning fluorimetry to detect ligand interactions that promote protein stability. Nat. Protoc. **2**:2212–2221.
34. **Ranjith-Kumar CT, Kao CC.** 2006. Biochemical activities of the HCV NS5B RNA-dependent RNA polymerase, p. 293–310. *In* Tan SL (ed), Hepatitis C viruses: genomes and molecular biology. Horizon Bioscience, Norfolk, United Kingdom.
35. **Reigadas S, et al.** 2001. HCV RNA-dependent RNA polymerase replicates in vitro the 3′ terminal region of the minus-strand viral RNA more efficiently than the 3′ terminal region of the plus RNA. Eur. J. Biochem. **268**:5857–5867.
36. **Rodriguez-Torres M, et al.** 2010. Safety and antiviral activity of the HCV non-nucleoside polymerase inhibitor VX-222 in treatment-naïve genotype 1 HCV-infected patients. Summ. 45th Annu. Meet. Eur. Assoc. Study Liver. EASL, Vienna, Austria. http://www.kenes.com/easl2010/orals/137.htm.
37. **Shi ST, et al.** 2009. Preclinical characterization of PF-00868554, a potent nonnucleoside inhibitor of the hepatitis C virus RNA-dependent RNA polymerase. Antimicrob. Agents Chemother. **53**:2544–2552.
38. **Tomei L, et al.** 2003. Mechanism of action and antiviral activity of benzimidazole-based allosteric inhibitors of the hepatitis C virus RNA-dependent RNA polymerase. J. Virol. **77**:13225–13231.
39. **Tomei L, et al.** 2004. Characterization of the inhibition of hepatitis C virus RNA replication by nonnucleosides. J. Virol. **78**:938–946.
40. **van Dijk AA, Makeyev EV, Bamford DH.** 2004. Initiation of viral RNA-dependent RNA polymerization. J. Gen. Virol. **85**:1077–1093.
41. **Wagner F, et al.** 2011. Antiviral activity of the hepatitis C virus polymerase inhibitor filibuvir in genotype 1-infected patients. Hepatology **54**: 50–59.
42. **Wang M, et al.** 2003. Non-nucleoside analogue inhibitors bind to an allosteric site on HCV NS5B polymerase. Crystal structures and mechanism of inhibition. J. Biol. Chem. **278**:9489–9495.